Chapter 12
Entropy Production-Based Closure of the Moment Equations for Radiative Transfer

Thomas Christen and Frank Kassubek

Abstract Heat radiation in gases or plasmas is usually out of local thermodynamic equilibrium (LTE) even if the underlying matter is in LTE. Radiative transfer can then be described with the radiative transfer equation (RTE) for the radiation intensity. A common approach to solve the RTE consists in a moment expansion of the radiation intensity, which leads to an infinite set of coupled hyperbolic partial differential equations for the moments. A truncation of the moment equations requires the definition of a closure. We recommend to use a closure based on a constrained minimum entropy production rate principle. It yields transport coefficients (e.g., effective mean absorption coefficients and Eddington factor) in accordance with the analytically known limit cases. In particular, it corrects errors and drawbacks from other closures often used, like the maximum entropy principle (e.g., the M1 approximation) and the isotropic diffusive P1 approximation. This chapter provides a theoretical overview on the entropy production closure, with results for an illustrative artificial example and for a realistic air plasma.

12.1 Introduction

Energy transfer by heat radiation in hot gases and plasmas is encountered in many different contexts like stellar and terrestrial atmospheres [1] and electric arcs [2], to mention a few examples. Although the energy carriers, the photons, do not interact with each other, the effective interaction due to scattering, emission, and absorption via the underlying matter makes the theoretical treatment of radiative

T. Christen (✉) · F. Kassubek
ABB Corporate Research, 5405 Dättwil, Switzerland
e-mail: thomas.christen@ch.abb.com

F. Kassubek
e-mail: frank.kassubek@ch.abb.com

R. C. Dewar et al. (eds.), *Beyond the Second Law*,
Understanding Complex Systems, DOI: 10.1007/978-3-642-40154-1_12,

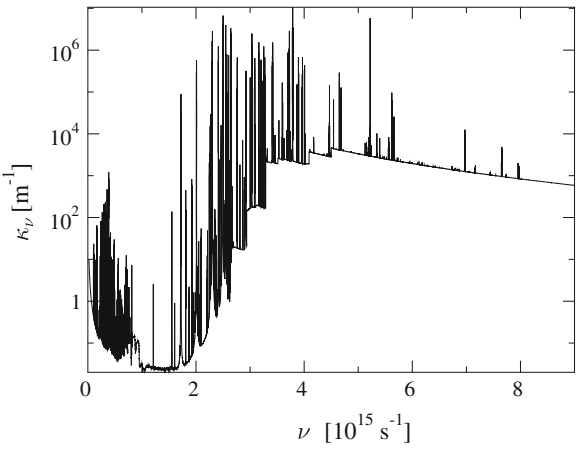

Fig. 12.1 Absorption spectrum of air plasma at 10,300 K and 2 bar [28], consisting of continuous bands (free-free, free-bound, bound-free transitions) superimposed to discrete peaks (bound-bound transitions) [29, 30]. The spectrum is not only a complicated function of frequency with huge variations ranging from 10^{-2} to 10^7 m^{-1}, but also strongly varies with temperature

transfer generally rather complicated [3]. In order to illustrate the possible complexity, the absorption spectrum κ_ν of air at about 10,000 K temperature is shown in Fig. 12.1. Here, κ_ν is the macroscopic spectral absorption coefficient in units of m^{-1}, and ν is the frequency. It consists of continuous bands and discrete peaks associated with electronic transitions of free-free, free-bound, and bound-bound states of the present air molecules, atoms, and ions.

An additional complication appears when the radiation is not in local thermal equilibrium (LTE). This is usually the case in gases and plasmas due to their partial transparency, even if the matter is in LTE. Non-LTE radiation refers to a photon distribution function n_ν that differs from the equilibrium Bose-Einstein or Planck distribution [4]

$$n_\nu^{(eq)} = \frac{1}{\exp(h\nu/k_B T) - 1}, \tag{12.1}$$

where h is the Planck constant, k_B the Boltzmann constant, and T the local temperature of the LTE matter.

For simplicity, we consider unpolarized radiation in an isotropic medium. The basic equation is then the radiative transfer equation (RTE) [1, 3] for the specific radiation intensity[1] [5]

$$I_\nu(\mathbf{x}, \Omega) = \frac{2h\nu^3}{c^2} n_\nu(\mathbf{x}, \Omega), \tag{12.2}$$

[1] In the following we will skip the term *specific*.

which describes the radiation flux at location $\mathbf{x}$ as a function of the direction Ω and frequency ν. The RTE reads

$$\frac{1}{c}\partial_t I_\nu + \Omega \cdot \nabla I_\nu = \mathscr{L}(B_\nu - I_\nu), \tag{12.3}$$

where $\mathscr{L}$ is linear in its argument $B_\nu - I_\nu$ (see discussion below) and can be expressed as

$$\mathscr{L}(B_\nu - I_\nu) = \kappa_\nu(B_\nu - I_\nu) + \sigma_\nu\left(\frac{1}{4\pi}\int_{S^2} d^2\tilde{\Omega}\, p_\nu\,(\Omega, \tilde{\Omega}) I_\nu(\tilde{\Omega}) - I_\nu\right). \tag{12.4}$$

The RTE can be transformed into a linear transport equation for n_ν by insertion of (12.2) in Eq. (12.3). It is a linear Boltzmann transport equation (see also [5] for further examples), where entropy production is caused uniquely by the term (12.4). Let us briefly explain the different terms of the RTE (see, e.g., [3]). The expression on the left hand side of Eq. (12.3) multiplied with c is the substantial derivative consisting of the explicit time derivative $\partial_t I_\nu$ plus the advection term $c\,\Omega \cdot \nabla$ due to the motion of the photons with speed c; $\Omega \cdot \nabla$ is the directional derivative. This net change of I_ν in direction of Ω must be equal to the sum of specific source and sink terms due to the radiation-matter interactions, written on the right hand side of Eq. (12.3) and detailed in Eq. (12.4). Photons are generated by emission and annihilated by absorption, expressed by $\kappa_\nu B_\nu$ and $\kappa_\nu I_\nu$, respectively. Here, B_ν is the Planck function for thermal equilibrium,

$$B_\nu = \frac{2h\nu^3}{c^2} n_\nu^{(eq)}. \tag{12.5}$$

By breaking time reversal symmetry, the "collision term" $\mathscr{L}(B_\nu - I_\nu)$ leads to the irreversibility that equilibrates nonequilibrium states, and is thus responsible for entropy production. The absorption coefficient κ_ν is generally a sum of products of particle densities, absorption cross-sections, and contains terms $1 - \exp(-h\nu/k_B T)$ [5]; it depends thus not only on frequency but also on the partial pressures of the present species, and the temperature. The expression (12.4) includes elastic scattering. Incoming photons of frequency ν from all directions $\tilde{\Omega}$ are scattered with probability $p_\nu(\Omega, \tilde{\Omega})$ into direction Ω. Among other properties [1], p_ν is assumed to be normalized according to $(4\pi)^{-1}\int_{S^2} d^2\tilde{\Omega}\, p_\nu(\Omega, \tilde{\Omega}) = 1$ with S^2 being the full solid angle 4π, and we denote by $d^2\Omega$ the (2-dimensional) volume angle increment. The strength of the scattering process is quantified by the spectral scattering coefficient σ_ν in units of m^{-1}. In the absence of any interaction, e.g., in vacuum or a fully transparent medium, the right hand side of Eq. (12.3) vanishes, which describes the so-called *(free) streaming limit*. In the particle picture it can be interpreted as the limit of ballistic propagation of the photons, i.e., propagation without any kind of scattering [6].

A number of procedures to solve the RTE exist [3]. In this chapter we discuss a simple but effective approach based on a truncated moment expansion with an

entropy production minimization closure [7, 8]. Kohler has shown that entropy production optimization principles hold for linearized Boltzmann transport equations [9–12]. He especially discusses the Boltzmann transport equation for gases and the transport of electrons in a solid near equilibrium. Note that the expression "near equilibrium" is used in this case for the linear nonequilibrium regime, i.e. where the linearization of the Boltzmann transport equation is an appropriate approximation. Far from equilibrium, however, higher order terms in the deviation $n_\nu - n_\nu^{(eq)}$ from equilibrium have to be taken into account, and the entropy production principle is no longer applicable. Because the RTE (12.3) for heat radiation has the form of a linearized Boltzmann transport equation, Kohler's argument applies here analogously (for similar transfer equations, see also [5, 6]). The "collision term" $\mathscr{L}(B_\nu - I_\nu)$ in Eq. (12.3) is indeed a linear function of $B_\nu - I_\nu$: if one replaces $-I_\nu$ by $B_\nu - I_\nu$ in the large bracket of the right hand side in Eq. (12.4), the additional terms associated with B_ν add up to zero because B_ν is independent of direction Ω. Because photons do not interact with each other, the RTE is exactly[2] linear over the *whole* nonequilibrium range, i.e., for arbitrarily large deviation $|B_\nu - I_\nu|$ from equilibrium. It has been conjectured [7] that this exact linearity of the RTE is the reason for the success of our approach discussed below also far from equilibrium.

This chapter is organized as follows. Section 12.2 defines the moments and their governing equations. In order to truncate the system of equations, a closure based on entropy production rate is introduced in Sect. 12.3. The main results are discussed and illustrated in Sect. 12.4. Some remarks on boundary conditions for the moments are provided in Sect. 12.5.

12.2 The Moment Equations for Radiative Transfer

The macroscopic radiative properties of highest interest are related to those quantities that occur in the hydrodynamic equations of the underlying matter. Those are energy density, energy flux, and radiation pressure, and can be obtained from $I_\nu(\Omega)$ by integration over frequency ν and angle Ω. One thus introduces the moments

$$E = \frac{1}{c}\int d\nu\, d^2\Omega\, I_\nu, \tag{12.6}$$

$$F_k = \frac{1}{c}\int d\nu\, d^2\Omega\, \Omega_k I_\nu, \tag{12.7}$$

[2] Three and more photon processes are disregarded.

$$\begin{aligned} \Pi_{kl} &= \frac{1}{c}\int dv\, d^2\Omega\, \Omega_k \Omega_l\, I_v, \\ \ldots &= \ldots, \end{aligned} \tag{12.8}$$

where $k, l = 1, \ldots, 3$ denote the three space directions. The integrations run from zero to infinity for v and over the whole solid angle (sphere S^2) for Ω. The list of moments continues with higher order moments $\Omega_k \Omega_l \ldots \Omega_N$ to infinite order. Multiplication of the RTE (12.3) with products and/or powers of Ω_k's, and integration over frequency and solid angle leads to the infinite set of equations

$$\frac{1}{c}\partial_t E + \nabla \cdot \mathbf{F} = P_E, \tag{12.9}$$

$$\begin{aligned} \frac{1}{c}\partial_t \mathbf{F} + \nabla \cdot \Pi &= \mathbf{P}_F, \\ \ldots &= \ldots, \end{aligned} \tag{12.10}$$

where $\mathbf{F}$ and Π denote the vector and the tensor with components given by Eqs. (12.7) and (12.8), respectively. The right hand sides are given by

$$P_E = \frac{1}{c}\int dv d^2\Omega \;\; \mathscr{L}(B_v - I_v) = \kappa_{\mathrm{E}}^{(\mathrm{eff})}(E^{(eq)} - E), \tag{12.11}$$

$$\begin{aligned} \mathbf{P}_F &= \frac{1}{c}\int dv d^2\Omega \;\; \Omega\, \mathscr{L}(B_v - I_v) = -\kappa_{\mathrm{F}}^{(\mathrm{eff})}\mathbf{F}, \\ \ldots &= \ldots, \end{aligned} \tag{12.12}$$

where

$$E^{(eq)} = \frac{4\pi}{c}\int_0^\infty dv\, B_{\boldsymbol{v}} = \frac{4\sigma_{SB}}{c}T^4 \tag{12.13}$$

is the LTE radiation energy density (σ_{SB} is the Stefan-Boltzmann constant), and for convenience the effective absorption coefficients $\kappa_{\mathrm{E}}^{(\mathrm{eff})}$ and $\kappa_{\mathrm{F}}^{(\mathrm{eff})}$ are introduced. In full equilibrium P_E and $\mathbf{P}_F$ vanish. The transport coefficients ($\kappa_{\mathrm{E}}^{(\mathrm{eff})}$, $\kappa_{\mathrm{F}}^{(\mathrm{eff})}$, …) are still functionals of the unknown function I_v. Once they are known, the moments (E, $\mathbf{F}$, …), which are the variables of the (still infinite) set of partial differential equations [(12.9), (12.10), ….], can be determined in principle by solving the latter, provided appropriate initial and boundary conditions are given.

For practical purposes, one has to truncate the set of equations and to restrict the model to a finite number N of moments. The equation for the highest order moment will then contain the moment of the subsequent order, which is not a variable, but an additional unknown quantity that depends on I_v. A closure method is a procedure that prescribes how to determine all these unknowns, which may eventually depend on all moments that are variables. In the following, we restrict ourselves to the two first moment equations (12.9) and (12.10) with variables E

and **F**, but we emphasize that our procedure is general and applicable to any order N of truncation.

Because the second rank tensor $\boldsymbol{\Pi}$ depends only on the scalar E and the vector **F**, it can be written by tensor symmetry reasons in the form

$$\Pi_{nm} = E\left(\frac{1-\chi}{2}\delta_{nm} + \frac{3\chi-1}{2}\frac{F_n F_m}{F^2}\right), \tag{12.14}$$

where the *variable Eddington factor* (VEF) χ is in general a function of E and $F = |\mathbf{F}|$, and δ_{kl} ($= 0$ if $k \neq l$ and $\delta_{kl} = 1$ if $k = l$) is the Kronecker delta. In thermal equilibrium all fluxes vanish, and the stress tensor is proportional to the unit tensor with diagonal elements $E^{(eq)}/3$. This follows from Eqs. (12.6) and (12.8), $|\Omega| = 1$ and the isotropy of the equilibrium radiation. Because we assume that the underlying matter is isotropic, the only distinguished direction is given by **F**, and $\kappa_E^{(\mathrm{eff})}(E, \mathrm{v})$, $\kappa_F^{(\mathrm{eff})}(E, \mathrm{v})$, and $\chi(E, \mathrm{v})$ can be expressed as functions of E and

$$\mathrm{v} = \frac{F}{E}. \tag{12.15}$$

Note that $0 \leq \mathrm{v} \leq 1$, with $\mathrm{v} = 1$ corresponding to the free streaming limit. v can be roughly understood as the dimensionless average velocity of the photon gas, where $\mathrm{v} = 1$ is associated with the speed of light c, which cannot be surpassed.

12.3 Closure by Entropy Production Rate Minimization

The task of the closure is to determine the transport coefficients, i.e., the effective or mean absorption coefficients $\kappa_E^{(\mathrm{eff})}$ and $\kappa_F^{(\mathrm{eff})}$, and the VEF χ as functions of E and v (or F). A closure that is often considered is based on entropy maximization [13–15] (and is in the present context sometimes named "M1-model"). However, Kohler [9] has proved validity of entropy production rate principles for the linearized Boltzmann transport equation. According to his results, near equilibrium the distribution function optimizes the entropy production rate under certain constraints, which are associated with fixed moments or fluxes. The type of the optimum, i.e., whether the optimum is a maximum or a minimum, depends on the specific choice of constraints. Kohler's proof has been re-discussed several times in the literature [10–12]. We mention also three additional works which indicate the relevance of entropy production principles for radiative transfer. Firstly, Essex [16] has shown that the entropy production rate is minimum in a grey atmosphere in local radiative equilibrium. Secondly, Würfel and Ruppel [17, 18] discussed entropy production rate maximization by introducing an effective chemical potential of the photons, related to their interaction with matter. Finally, Santillan et al. [19] showed that for a constraint of fixed radiation power, black bodies maximize the entropy production rate.

The closure procedure based on entropy production minimization has been outlined for photons in [7, 8], and for a gas of independent electrons in [20]. The receipt, in a nutshell, is to minimize the entropy production rate, which is a functional of I_ν, subject to the constraints of fixed moments (given by Eqs. (12.6), (12.7) etc.). The result of this optimization problem will then be a function $I_\nu(E, \mathbf{F})$, from which all unknowns (P_E, $\mathbf{P}_F$, ...) can be determined. In order to derive the expression for the entropy production rate, we start with the entropy per volume of the photon gas [4, 21, 22]

$$S_{\text{rad}}[I_\nu] = -k_B \int d^2\Omega\, d\boldsymbol{\nu}\, \frac{2\nu^2}{c^3}\left(n_\nu \ln n_\nu - (1+n_\nu)\ln(1+n_\nu)\right), \tag{12.16}$$

where Eq. (12.2) relates n_ν to I_ν. The total entropy production rate, $\sum$, consists of the two contributions $\sum_{\text{rad}}$ and $\sum_{\text{mat}}$ associated with entropy production in the photon gas and in the matter, respectively (cf. [23]). The contribution $\sum_{\text{rad}}$ is obtained from the time-derivative of Eq. (12.16), by making use of Eq. (12.3), and writing the result in the form $\partial_t S_{\text{rad}} + \nabla \cdot \mathbf{J}_S = \sum_{\text{rad}}$, which yields

$$\sum\nolimits_{\text{rad}}[I_\nu] = -k_B \int d\nu\, d^2\Omega\, \frac{1}{h\nu} \ln\left(\frac{n_\nu}{1+n_\nu}\right) \mathscr{L}(B_\nu - I_\nu); \tag{12.17}$$

here $\mathbf{J}_S$ is the entropy current density.

The second contribution, the entropy production rate of the LTE matter, $\sum_{\text{mat}}$, can be derived from the fact that the matter can be considered locally as an equilibrium bath with temperature $T(\mathbf{x})$. Energy conservation implies that the local power production W of the matter is related to the radiation power density in Eq. (12.11) by $W = -cP_E$. The entropy production rate (associated with radiation) in the local heat bath is thus $\sum_{\text{mat}} = W/T = -cP_E/T$. Equation (12.1) implies $h\nu/k_B T = \ln(1 + 1/n_\nu^{(eq)})$, and one obtains with Eq. (12.11)

$$\sum\nolimits_{\text{mat}}[I_\nu] = -k_B \int d\nu d^2\Omega\, \frac{1}{h\nu} \ln\left(\frac{1+n_\nu^{(eq)}}{n_\nu^{(eq)}}\right) \mathscr{L}(B_\nu - I_\nu)\ . \tag{12.18}$$

The total entropy production rate $\sum = \sum_{\text{rad}} + \sum_{\text{mat}}$ becomes

$$\sum[I_\nu] = -k_B \int d\nu d^2\Omega\, \frac{1}{h\nu} \ln\left(\frac{n_\nu(1+n_\nu^{(eq)})}{n_\nu^{(eq)}(1+n_\nu)}\right) \mathscr{L}(B_\nu - I_\nu)\ . \tag{12.19}$$

This quantity has to be minimized by varying I_ν and considering the constraints given by Eqs. (12.6) and (12.7) with E, $\mathbf{F}$ kept fixed. One has thus to solve

$$\frac{\delta}{\delta I_\nu}\left[\sum[I_\nu] - \lambda_E\left(E - \frac{1}{c}\int d\nu\, d^2\Omega\, I_\nu\right) - \lambda_{\mathbf{F}} \cdot \left(\mathbf{F} - \frac{1}{c}\int d\nu\, d^2\Omega\, \Omega\, I_\nu\right)\right] = 0 \tag{12.20}$$

for I_ν, where the Lagrange multipliers λ_E and λ_F can be eliminated with the help of Eqs. (12.6) and (12.7), which leads then to $I_\nu(\Omega, E, \mathbf{F})$. We mention that in the entropy maximization closure Σ is replaced by S_{rad} given by Eq. (12.16).

12.4 Results

In the following, we will not re-iterate the analytical calculations reported in [7, 8], but immediately discuss the results $\kappa_E^{(\text{eff})}(E, \text{v})$, $\kappa_F^{(\text{eff})}(E, \text{v})$, and $\chi(E, \text{v})$ as functions of E and v, and explain their properties for simple illustrative cases.

12.4.1 Equilibrium Limit

If the radiation field (or photon gas) is in LTE with the matter ($I_\nu = B_\nu$), all transport properties can be obtained by considering the leading order deviations from LTE, $\delta I_\nu = I_\nu - B_\nu$, $\delta E = E - E^{(eq)}$, and $\delta F = F$. A corresponding expansion and subsequent solution of the minimization problem (12.20) leads then to [7, 8]

$$\kappa_E^{(\text{eff})} = \langle \kappa_\nu \rangle_{\text{Ro}}, \tag{12.21}$$

$$\kappa_F^{(\text{eff})} = \langle \kappa_\nu + \sigma_\nu \rangle_{\text{Ro}}, \tag{12.22}$$

$$\chi = \frac{1}{3}, \tag{12.23}$$

where the Rosseland average of any spectral function h_ν is defined by

$$\langle h_\nu \rangle_{\text{Ro}} := \frac{\int_0^\infty \mathrm{d}\nu\, \nu^4 \partial_\nu n_\nu^{(eq)}}{\int_0^\infty \mathrm{d}\nu\, \nu^4 h_\nu^{-1} \partial_\nu n_\nu^{(eq)}}, \tag{12.24}$$

with ∂_ν being frequency differentiation. If h_ν is a physical rate (per time or per length) the Rosseland mean is the inverse of an average of inverse rates. Thus, frequencies with small κ_ν-values are dominating the Rosseland average, due to a macroscopic number of absorption-emission events (on the considered length scale). In order to establish LTE with matter, the medium must behave optically dense. The result (12.23) means that the stress tensor $\boldsymbol{\Pi}_{kl} = (E/3)\delta_{kl}$ is associated with isotropic radiation.

These LTE results are well-known and can be obtained also with other procedures [3]. Every reasonable closure to the moment equations should provide Eqs. (12.21)–(12.23). The often considered maximum entropy closure is incorrect near equilibrium as has been pointed out by Struchtrup [23]. For LTE, it is obvious

from Kohler's work [9], that the entropy production rate is the appropriate quantity to be optimized.

12.4.2 Emission Limit

In this limit emission strongly predominates absorption. It is characterized by very low radiation intensity, $I_\nu \ll B_\nu$, such that $E \ll E^{(eq)}$, and is thus far from equilibrium. One can also derive analytical expressions for the transport coefficients [8] by an expansion in terms of the small quantities I_ν, E, and F. Entropy production minimization gives [7, 8]

$$I_\nu = \frac{2k_B}{c}\frac{v^2\kappa_\nu}{\lambda_E + \lambda_\mathbf{F}\cdot\Omega} n_\nu^{(eq)}, \tag{12.25}$$

where the Lagrange multipliers are related to E and F by

$$E = \frac{k_B\mathscr{T}(\kappa_\nu)}{c^2\lambda_F}\ln\left(\frac{\lambda_E+\lambda_F}{\lambda_E-\lambda_F}\right), \tag{12.26}$$

$$F = \frac{k_B\mathscr{T}(\kappa_\nu)}{c^2\lambda_F}\left(2-\frac{\lambda_E}{\lambda_F}\ln\left(\frac{\lambda_E+\lambda_F}{\lambda_E-\lambda_F}\right)\right). \tag{12.27}$$

Here, we introduced the integral

$$\mathscr{T}(h_\nu) = 4\pi\int_0^\infty \mathrm{d}v\, v^2 h_\nu n_\nu^{(eq)} \tag{12.28}$$

for frequency dependent functions h_ν. The transport coefficients are given by [8]

$$\kappa_E^{(\mathrm{eff})} = \langle\kappa_\nu\rangle_{\mathrm{Pl}}, \tag{12.29}$$

$$\kappa_F^{(\mathrm{eff})} = \frac{\mathscr{T}(\kappa_\nu(\kappa_\nu+\sigma_\nu))}{\mathscr{T}(\kappa_\nu)}, \tag{12.30}$$

$$\chi(\mathrm{v}) = -\frac{\lambda_E}{\lambda_F}\mathrm{v}, \tag{12.31}$$

where

$$\langle h_\nu\rangle_{\mathrm{Pl}} = \frac{\int_0^\infty \mathrm{d}v\, v^3 h_\nu n_\nu^{(eq)}}{\int_0^\infty \mathrm{d}v\, v^3 n_\nu^{(eq)}} \tag{12.32}$$

is the so-called Planck average of a frequency dependent function h_ν. Contrary to the opaque near-equilibrium limit [see Eq. (12.24)] from the previous subsection,

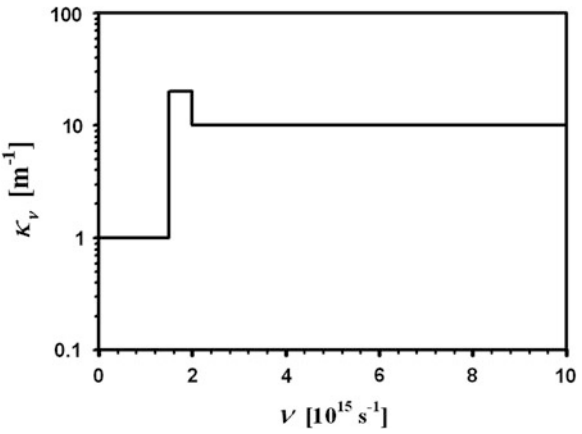

Fig. 12.2 Artificial spectrum with low absorption below a threshold frequency (1.5 PHz) and high absorption above, with an intermediate maximum below 2 PHz

in the transparent emission limit the effective absorption coefficients are averages (12.32) of the direct rates, rather than averages of inverse rates.

The VEF can easily be numerically calculated from the above equations. For small v, an expansion of Eqs. (12.26) and (12.27) gives $\lambda_E/\lambda_F = -1/(3\mathrm{v})$, in accordance with the isotropic limit. In the free streaming limit, $\mathrm{v} \to 1$ from below, one can show that $\lambda_F \to -\lambda_E$ [8], as one expects that $\chi \to 1$.

12.4.3 General Case

For arbitrary values of E and v (or F) the radiation intensity and the transport coefficients must be numerically computed. For use in radiation simulations, it is thus necessary to calculate the transport coefficients for real gases and plasmas and tabulate them as functions of all variables, including temperature and pressure of the LTE matter. In the following, we first consider an illustrative artificial example with negligible scattering ($\sigma_\nu \equiv 0$) and an absorption spectrum shown as in Fig. 12.2. In a frequency band below a certain threshold absorption is low, while at the threshold frequency absorption strongly increases to a maximum, beyond which it again decays or remains constant. The entropy production approach then leads to radiation intensities I_ν plotted in Fig. 12.3. The equilibrium radiation associated with $E = E^{(eq)}$ and $\mathrm{v} = 0$ corresponds to the well-known Planck distribution (solid curve). Nonequilibrium occurs if $E \neq E^{(eq)}$ or $\mathrm{v} \neq 0$. Consider first an isotropic nonequilibrium state where the energy of the radiation is smaller than the equilibrium energy, for instance $E = E^{(eq)}/2$ and $\mathrm{v} = 0$. According to the figure, the radiation (dashed curve) is the closer to equilibrium the larger the absorption constant is. The same holds for the contrary case where the radiation energy is above the equilibrium value ($E = 2E^{(eq)}$ and $\mathrm{v} = 0$, dotted curve). Because the magnitude of the absorption constant is a measure for the interaction

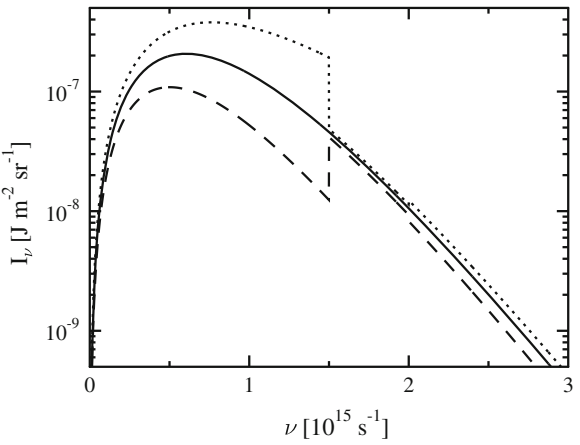

Fig. 12.3 Radiation intensities I_ν for $\mathrm{v} = 0$, $T = 10,300$ K and different values of $E/E^{(eq)}$ and the spectrum given in Fig. 12.2. For $E/E^{(eq)} = 1$ (*solid curve*), equilibrium radiation is established (Planck distribution). For other $E/E^{(eq)}$ values (*dotted* $E/E^{(eq)} = 2$; *dashed* $E/E^{(eq)} = 0.5$), non-equilibrium occurs with a strength that is related to the magnitude of κ_ν. The larger κ_ν, the stronger is equilibration

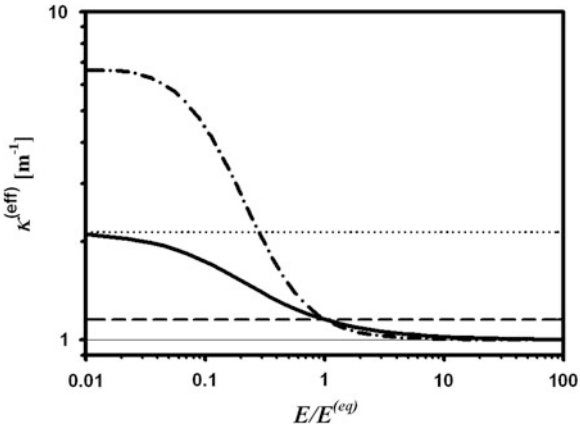

Fig. 12.4 Effective absorption coefficients $\kappa_E^{(\mathrm{eff})}$ (*solid*) and $\kappa_F^{(\mathrm{eff})}$ (*dashed-dotted*) as functions of the radiation energy for $\mathrm{v} = 0$, for the spectrum shown in Fig. 12.2. The Planck mean, Rosseland mean, and minimum of κ_ν are indicated by the *dotted*, *dashed*, and *thin solid lines*

strength between radiation and matter, this behaviour reflects the fact that photons with more intensive interaction with LTE matter are more efficiently equilibrated. Entropy production rate optimization principles inherently take this general tendency into account [24]. For $\mathrm{v} \neq 0$, the intensity I_ν depends on Ω [see, e.g., Eq. (12.25)]; details will not be discussed here.

The mean absorption coefficients are shown in Fig. 12.4. The different limit cases discussed in the previous subsections are indicated by horizontal lines. At equilibrium, all effective absorption coefficients equal the Rosseland mean.

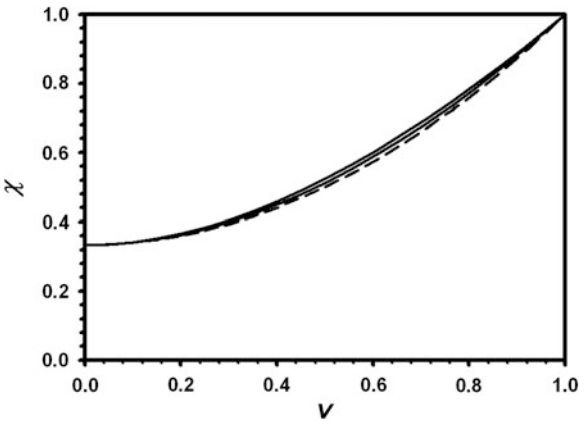

Fig. 12.5 *Solid curves*: The Eddington factor $\chi(\mathrm{v})$ for the spectrum in Fig. 12.2 for two different values $E/E^{(eq)} = 1$ (*lower solid curve*) and 0.5 (*upper solid curve*). *Dashed*: Kershaw approximation Eq. (12.33)

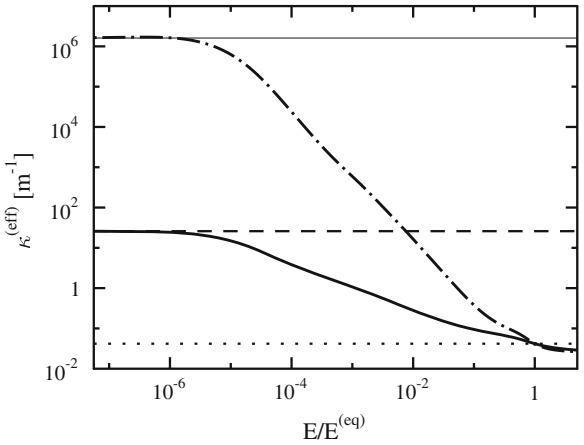

Fig. 12.6 Effective absorption coefficients $\kappa_E^{(\mathrm{eff})}$ (*solid*) and $\kappa_F^{(\mathrm{eff})}$ (*dashed-dotted*) for an air plasma at 10,000 K and 2 bar (see Fig. 12.1) as functions of the radiation energy for $\mathrm{v} = 0$. The Planck mean, Rosseland mean, and emission limit for $\kappa_F^{(\mathrm{eff})}$ from Eq. (12.30) are indicated by the *dashed*, *dotted*, and *thin solid lines*

A closure by entropy maximization would provide a wrong result [7, 8]. We note also that for $E/E^{(eq)} \to \infty$, the entropy production closure leads to a mean absorption dominated by the minimum absorption coefficient. In this limit the overwhelming amount of photons will occupy states with low photon-matter interaction, while the states with stronger interaction (large absorption) will be near the equilibrium distribution.

The VEF as a function of v is shown in Fig. 12.5 for two different E-values. It can be shown that the VEF satisfies a number of conditions [14]. For instance, as mentioned $\chi = 1/3$ for $\mathrm{v} = 0$ (isotropic radiation) and $\chi = 1$ for $\mathrm{v} = 1$ (free streaming limit). Furthermore, the dependence of χ on E is weak, and for many practical purposes $\chi(\mathrm{v})$ is well approximated by Kershaw's VEF [25]

$$\chi = \frac{1 + 2\mathrm{v}^2}{3}, \tag{12.33}$$

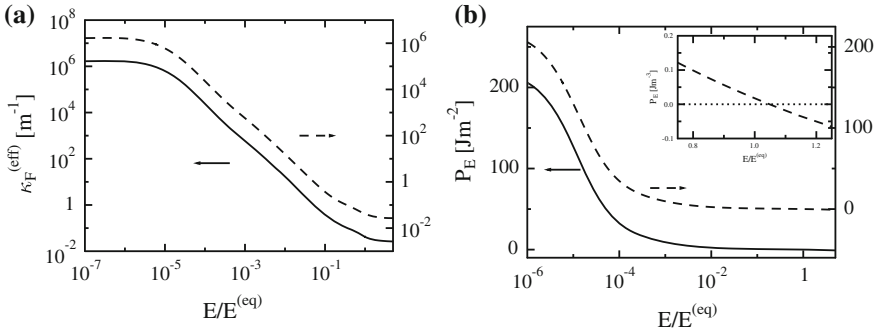

Fig. 12.7 *Left*: Effective absorption coefficient $\kappa_F^{(\mathrm{eff})}$ as a function of radiation energy for $\mathrm{v} = 0$ (*solid line*, left axis) and $\mathrm{v} = 0.2$ (*dashed line*, right axis) *Right*: Absorption power P_E as a function of radiation energy for $\mathrm{v} = 0$ (*solid line*, left axis) and $\mathrm{v} = 0.2$ (*dashed line*, right axis). The inset shows the shift of the zero of P_E from $E/E^{(eq)} = 1$; because of this shift it is inconvenient to directly discuss κ_E, as it is defined here, in a graph

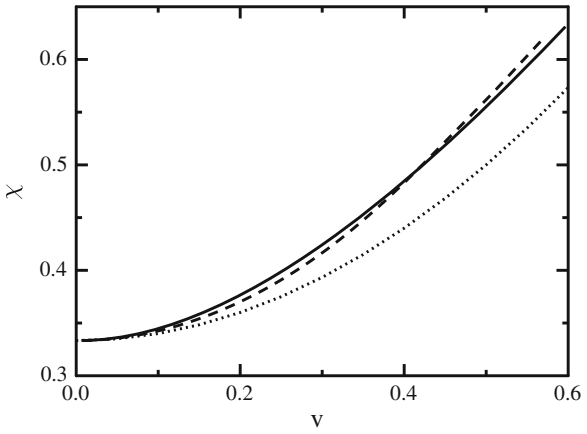

Fig. 12.8 Variable Eddington factor (VEF) for the air spectrum as a function of v for $E/E^{(eq)} = 1$ (*solid*) and $E/E^{(eq)} = 1/4$ (*dashed*). Kershaw's VEF is given as a reference (*dotted*)

as is illustrated also in Fig. 12.5.

This general behaviour of the transport coefficients observed for the toy example is also valid for more complex absorption spectra. A calculation with a spectrum as given by Fig. 12.1 (air plasma at 10,000 K and 2 bar) has to take into account the small structures from the individual spectral lines and requires a rather high-frequency resolution. As a side remark, we mention an additional difficulty as there is a critical value of the Lagrange multiplier λ_F (for given λ_E) for which the solution of the variational equation (12.20) becomes singular. Even for this value, however, $\mathrm{v} < 1$ and hence in order to go to the streaming limit, the intensity distribution acquires a δ-function contribution: part of the photons then concentrate (condense) at the frequency with minimal κ_ν in the streaming direction.

Details of the behaviour at large v will be described elsewhere, here we restrict ourselves to sufficiently small v-values. The effective absorption coefficients for $v = 0$ are shown in Fig. 12.6. The span over several orders of magnitude between the emission limit and a dense medium is remarkable. We mention that the detailed slightly wavy structures of $\kappa_E^{(\mathrm{eff})}$ and $\kappa_F^{(\mathrm{eff})}$ are not due to numerical inaccuracy but due to the specific frequency dependence of the absorption spectrum.

The numerical solutions show that the v dependence of the effective absorption coefficients is rather weak. In Fig. 12.7, a comparison between $v = 0$ and $v = 0.2$ is shown as an example. For practical use it is much more convenient to depict P_E instead of κ_E, because for finite v the zero of P_E is shifted away from $E = E^{(eq)}$ (cf. definition of κ_E by Eq. (12.11) and inset in Fig. 12.7).

On the other hand, the VEF depends relatively weakly on the energy of the radiation field. Fig. 12.8 shows χ for two different energies as an example.

12.5 Boundary Conditions

In order to have a well-defined hyperbolic problem associated with the partial differential equations (PDEs) (12.9) and (12.10), appropriate boundary conditions on E and $\mathbf{F}$ (or $\mathbf{v}$), at solid surfaces, at certain symmetry planes, and/or at infinity must be added. The qualitative nature of the boundary depends not only on the radiative behavior of the matter but also on the direction of the characteristics of the basic PDEs. This is analogous to gas dynamics, where a boundary condition at an outlet is needless if the Mach number of the flow is larger than one, because no information can travel from the boundary back into the system. For the Eqs. (12.9) and (12.10), this appears if v is larger than a critical value v_c. This value depends on the functional dependence of χ on v, but is typically around 0.7 [8]. If boundary conditions are needed for moment equations, they can be derived by projection of $I_\nu(\Omega)$, expanded in terms of the moments, onto a weight function. Often, the Marshak boundary condition is considered, which can be generalized in the present case to [8]

$$F = \frac{\varepsilon}{2(2-\varepsilon)}\left(E_\mathrm{w} - \frac{(3+15\chi)E}{8}\right), \tag{12.34}$$

where ε is the surface emittance, and E_w is the equilibrium radiation energy density associated with the wall temperature. In the equilibrium limit ($\chi = 1/3$), Eq. (12.34) reduces to the usual Marshak boundary condition, as applied, for instance, in the diffusive P1-model [26].

In cases where the surface response to radiation is relevant and a good modelling of the surface behavior is crucial (e.g., if radiation-induced material ablation occurs), it may be more appropriate to include a solid surface layer in the simulation domain with realistic absorption and scattering coefficients [8].

12.6 Summary and Conclusion

We conclude that the entropy production rate is an appropriate variational functional for the closure of the moment equations of radiative transfer. Within the formalism, effective absorption coefficients and variable Eddington factors are calculated that have the correct limiting behavior in the analytically known cases, like the Planck and Rosseland mean absorption, and the VEF in the diffusive and free streaming limits. It turns out that the entropy production principle is superior to the often considered entropy maximization principle, which disregards the specific equilibration mechanisms and yields in general wrong results even in the Rosseland (equilibrium) limit, as has been extensively discussed in general in [23] and for specific examples in [7, 8]. As demonstrated with a toy example and a calculation for a realistic spectrum of air, the effective absorption coefficients can vary over several orders of magnitude in the physically relevant region. This shows that good models are necessary.

The success of the entropy production approach is related to Kohler's principle [9], because the linearity of the RTE is exact and not restricted to a linearization region near equilibrium. From the formalism discussed it is obvious that the approach is not limited to a specific number of moments, and it is applicable to other types of mutually non-interacting particles like neutrinos [27] or independent electrons [20].

References

1. Chandrasekhar, S.: Radiative Transfer. Dover Publ. Inc, New York (1960)
2. Jones, G.R., Fang, M.T.C.: The physics of high-power arcs. Rep. Prog. Phys. **43**, 1415 (1980)
3. Siegel, R., Howell, J.R.: Thermal Radiation Heat Transfer. Washington, Philadelphia (1992)
4. Landau, L.D., Lifshitz, E.M.: Statistical Physics. Elsevier, Amsterdam (2005)
5. Tien, C.L,: Radiation properties of gases. In: Irvine Jr, T.F, Hartnett, J.P (eds.) Advances in heat transfer, vol. 5. Academic Press, Inc., New York, 253 (1968)
6. Chen, G.: Nanoscale Energy Transport and Conversion: A Parallel Treatment of Electrons, Molecules, Phonons, and Photons. Oxford University Press, USA (2005)
7. Christen, T., Kassubek, F.: Minimum entropy production closure of the photo-hydrodynamic equations for radiative heat transfer. J. Quant. Spectrosc. Radiat. Transfer. **110**, 452 (2009)
8. Christen T, Kassubek F, and Gati R.: Radiative heat transfer and effective transport coefficients. In: Aziz Belmiloudi (ed.) Heat Transfer—Mathematical modelling, numerical methods and information technology, InTech, Rijeka, Croatia (2011)
9. Kohler, M.: Behandlung von Nichtgleichgewichtsvorgängen mit Hilfe eines Extremalprinips. Z. Physik **124**, 772 (1948)
10. Ziman, J.M.: The general variational principle of transport theory. Can. J. Phys. **34**, 1256 (1956)
11. Ziman, J.M.: Electrons and Phonons. Clarendon Press, Oxford (1967)
12. Martyushev, L.M., Seleznev, V.D.: Maximum entropy production principle in physics, chemistry, and biology. Phys. Rep. **426**, 1 (2006)
13. Minerbo, G.N.: Maximum entropy Eddington factors. J. Quant. Spectrosc. Radiat. Transfer. **20**, 541 (1978)

14. Levermore, C.D.: Moment closure hierarchies for kinetic theories. J. Stat. Phys. **83**, 1021 (1996)
15. Turpault, R.: A consistent multigroup model for radiative transfer and its underlying mean opacities. J. Quant. Spectrosc. Radiat. Transfer. **94**, 357 (2005)
16. Essex, C.: Minimum entropy production in the steady state and radiative transfer. The Astrophys. J. **285**, 279 (1984)
17. Würfel, P., Ruppel, W.: The flow equilibrium of a body in a radiative field. J. Phys. C: Solid State Phys. **18**, 2987 (1985)
18. Kabelac, S.: Thermodynamik der Strahlung. Vieweg, Braunschweig (1994)
19. Santillan, M., de Parga, G.A., Angulo-Brown, F.: Black-body radiation and the maximum entropy production regime. Eur. J. Phys. **19**, 361 (1998)
20. Christen, T.: Nonequilibrium distribution function and generalized hydrodynamics for independent electrons from an entropy production rate principle. Europhys. Lett. **89**, 57007 (2010)
21. Oxenius, J.: Radiative transfer and irreversibility. J. Quant. Spectrosc. Radiat. Transfer **6**, 65 (1966)
22. Kröll, W.: Properties of the entropy production due to radiative transfer. J. Quant. Spectrosc. Radiat. Transfer **7**, 715 (1967)
23. Struchtrup H.: Rational extended thermodynamics. Müller I and Ruggeri T. (ed.) p. 308. Springer, New York, Second Edition (1998)
24. Christen, T.: Modeling electric discharges with entropy production rate principles. Entropy **11**, 1042 (2009)
25. Kershaw D, *Flux limiters nature's own way* Lawrence Livermore Laboratory UCRL-78378 (1976)
26. Nordborg, H., Iordanidis, A.: Self-consistent radiation based modelling of electric arcs: I. Efficient radiation approximations. J. Phys. D Appl. Phys. **41**, 135205 (2008)
27. Essex C and Kennedy DC J. Stat. Phys. **94**, 253 (1999). (or Minimum entropy production of neutrino radiation in the steady state, Report No: DOE/ER/40272-280 UFIFT-HEP-97- 7)
28. Data for the air spectrum has been provided by R. Gati (ABB Corporate Research) with use of tools by V. Aubrecht
29. Aubrecht, V., Lowke, J.J.: Calculations of radiation transfer in SF6 plasmas using the method ofpartial characteristics. J. Phys. D Appl. Phys. **27**, 2066 (1994)
30. Chaveau, S., et al.: Radiative transfer in LTE air plasmas for temperatures up to 15,000 K. J. Quant. Spectrosc. Radiat. Transfer. **77**, 113 (2003)